Structural Engineering and Mechanics, Vol. 4, No. 3 (1996) 330-344
DOI: http://dx.doi.org/10.12989/sem.1996.4.3.330

Dry friction losses in axially loaded cables

Xiaolun Huang†

Wittke Waste Equipment, Medicine Hat, AB, T1C 1K6 Canada

Oleg G. Vinogradov‡

Department of Mechanical Engineering, University of Calgary, Calgary, AB, T2N 1N4 Canada

Abstract. A model of a cable comprising interacting wires with dry friction forces at the interfaces is subjected to a quasi-static cyclic loading. The first cycle of this process, comprising of axial loading, unloading and reloading is investigated analytically. Explicit load-elongation relationships are obtained for all of the above phases of the cycle. An expression for the hysteretic losses is also obtained in an explicit form. It is shown that losses are proportional to the third power of the amplitude of the oscillating axial force, and are in inverse proportion to the interwire friction forces. The results obtained are used to introduce a model of a cable as a solid rod with an equivalent stiffness and damping properties of the rod material. It is shown that the stiffness of the equivalent rod is weakly nonlinear, whereas the viscous damping coefficient is proportional to the amplitude of the oscillation. Some numerical results illustrating the effect of cable parameters on the losses are given.

Key words: cable mechanics; cyclic loading; dry friction; hysteresis.

1. Introduction

A model of a cable comprising interacting wires in which a slip between the wires is allowed was considered by the authors for the case of extension of an initially pre-stretched cable (Huang and Vinogradov 1994). It was shown in that paper that losses in a cable caused by dry friction occur due to twisting and bending of individual wires. The effect of twisting of wires on the losses in a bent cantilever cable was considered by Vinogradov and Atatekin (1986). More recently, such an effect in an axially loaded and uniformly bent cable was investigated by Huang and Vinogradov (1992, 1994).

In this paper the results obtained by Huang and Vinogradov (1996) for the case of loading are extended to include two other phases of a cycle: unloading and reloading. The full investigation of the cycle results in a hysteretic curve characterising the structural losses in a cable. The load-elongation relationships during the cycle, obtained in an analytical form, allowed to derive an explicit expression for the structural losses.

The analytical form of the load-elongation relationship is used to introduce a model of a cable as a solid rod with some dynamically equivalent properties of the rod material: equivalent stiffness and damping.

† Mechanical Engineer
‡ Professor

Some numerical results are given to illustrate the behaviour of the cable during the cycle of loading and the dependence of losses on cable parameters.

2. Hysteresis

The beginning of a cyclic loading is characterised by three phases: loading, unloading and reloading. The result of the first cycle is the hysteretic loop formed during the unloading and reloading phases of the cycle. However, to find out the hysteretic behaviour, the load-elongation characteristics during the entire first cycle must be analyzed. The behaviour of a tension cable in the loading phase was considered in the preceding paper by Huang and Vinogradov (1996). In this paper the treatment of the unloading and reloading phases is based on the results obtained for the loading phase. Specifically, the two other phases of the cycle are considered as "loading" with respect to different initial states of the cable. Thus the problem is solved as an initial value problem, that is, the state of the cable at the end the loading phase becomes an initial state for the unloading one, and so on. For this reason, the state of the cable at the end of the loading phase is presented briefly first. For the details the reader is referred to Huang and Vinogradov (1996). Note, that the parameters related to the three phases of a cycle are identified by the subscripts 1, 2 and 3, for loading, unloading and reloading phases, respectively.

2.1. Loading

A cable, consisting of a core and n helical wires, is clamped at both ends against self-loosening rotation and is subjected to axial extension. Due to the structural symmetry only a half of the cable is analyzed. It is assumed that, in general, at the end of the loading phase the cable comprises two parts: one (H_s) in which the macro-slip took place, and another one (H_n) where a micro-slip but not the macro-slip was in presence (see Fig. 1(a) and (b), where a half-length of the cable is considered). The length of the slipping region during the loading is proportional to the axial load (Huang and Vinogradov 1996).

$$G_{s1}=\frac{GP_1}{p_f} \tag{1}$$

where G is a cable structural parameter. The helix angle in the slipping part varies linearly along the cable length according to the following relationship

$$\alpha_{s1}=\alpha_{n1}+\frac{Dp_f}{\sin\alpha_0}(z-H+H_{n1}),\quad H-H_{n1}\le z\le H \tag{2}$$

whereas in the nonslipping part of the cable, the helix angle is given by

$$\alpha_{n1}=\alpha_0+C(P-nm_n\cos\alpha_0), \tag{3}$$

where α_0 is the initial helix angle, C and D are the structural parameters, K_n is the stiffness of the cable as a solid rod, and p_f and m_n are the distributed interwire friction force and moments, respectively. A sketch of the variability of the helix angle along the cable at the intermediate state of the loading phase is shown in Fig. 1(b).

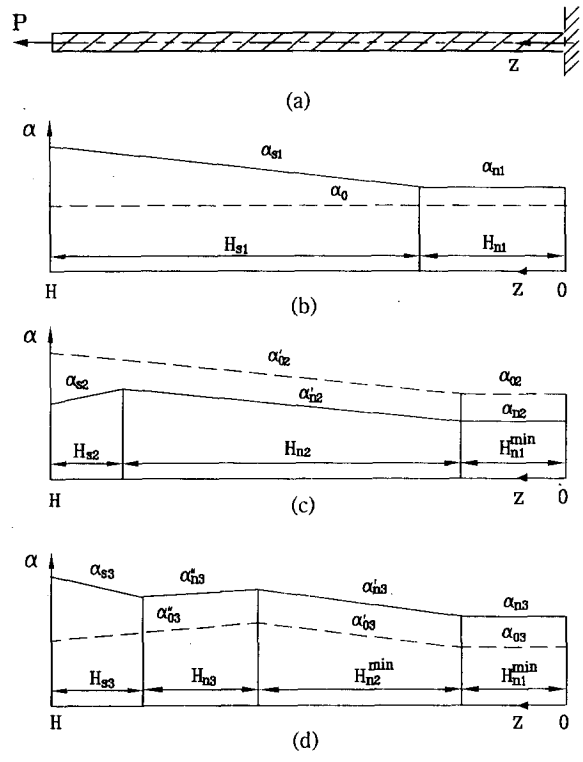

Fig. 1 Variability of helix angle along the half-length of cable at variousphases of cyclic loading. (a) half-length of cable; (b) loading phase; (c)unloading phase; (d) reloading phase.

When the axial load is such that $0<P_1<nm_n\cos\alpha_0$, the cable elongation is given by Huang and Vinogradov (1996).

$$\delta_1=\frac{4}{\sin 2\alpha_0}\left(\int_0^H \Delta\alpha_n dz+\int_0^{H_s}\Delta\alpha_s dz\right) \tag{4}$$

where $\Delta\alpha_n=0.5\sin 2\alpha_0(P_1/K_n)$. The integration in the latter yields

$$\delta_1=\frac{2H}{K_n}P_1+\frac{Dp_f}{\sin^2\alpha_0\cos\alpha_0}H_{s1}^2 \tag{5}$$

When $P_1>nm_n\cos\alpha_0$, the elongation of the cable is represented by Huang and Vinogradov (1996)

$$\delta_1=\frac{2H}{K_n}nm_n\cos\alpha_0+\frac{4}{\sin 2\alpha_0}\left(\int_0^H \Delta\alpha_{m1}dz+\int_{H_{n1}}^H \Delta\alpha_{s1}dz\right) \tag{6}$$

which, after integration, gives,

$$\delta_1=\frac{2H}{K_n}nm_n\cos\alpha_0+\frac{4HC}{\sin 2\alpha_0}(P_1-nm_n\cos\alpha_0)+\frac{DG^2}{\sin^2\alpha_0\cos\alpha_0}\frac{P_1^2}{p_f} \tag{6'}$$

Eq. (6') shows that, since $d^2\delta_1/dP_1^2>0$, the load-elongation curve $\delta_1=\delta_1(P_1)$ is concave (correspondingly, $P_1=P_1(\delta_1)$ is convex).

2.2. Unloading

The unloading is considered as a process of loading which starts at the end of the loading phase and during which the load changes according to the following relationship

$$P_2 = P^{\max} + P'_2 \qquad 0 \le P_2 \le P^{\max} \tag{7}$$

where $P^{\max}$ is the amplitude of the cyclic tension force, and P'_2 is the relative load in the unloading phase, $-P^{\max} \le P'_2 \le 0$.

The state of the cable at the end of the loading phase is thus the initial state for the following unloading phase. Under the action of a compressive load, a slip in the direction opposite to that of the loading phase will start again at the extended ends of the cable. As a result, the cable at any intermediate state of unloading will have three distinguished segments (see Fig. 1c):

(1) a uniform segment whose length is equal to the micro-slipping segment at the end of stage one, denoted by $H_{n1}^{\min}$;

(2) a new non-slipping or micro-slipping segment (depending on the amplitude of the relative load), with respect to the state of the cable at the end of stage one, denoted by H_{n2}, and

(3) a new reverse slipping segment H_{s2}. It is seen from Fig. 1(c) that H_{n2} is related to H_{s2} by

$$H_{n2} = H_{s1}^{\max} - H_{s2} \tag{8}$$

The objective of the following analysis is to find a relationship between the relative axial force P'_2 and the corresponding relative elongation of the cable. This can be done by following the same procedures as outlined for the loading phase (Huang and Vinogradov 1996).

Consider the helix angle first. At the beginning of the unloading phase, the helix angles in different segments should be equal to those at the end of the loading phase, i.e. from Eqs. (2) and (3),

$$\alpha_{02} = \alpha_0 + C(P^{\max} - nm_n \cos\alpha_0), \qquad 0 \le z \le H_{n1}^{\min} \tag{9}$$

$$\alpha'_{02} = \alpha_{02} + \frac{Dp_f}{\sin\alpha_0}(z - H + H_{n1}^{\min}), \qquad H - H_{n1}^{\min} \le z \le H \tag{10}$$

where α_{02} and α'_{02} are the initial helix angles in the micro-slipping and macro-slipping parts of the cable at the beginning of unloading, respectively.

When the amplitude of P'_2 is so small that there is no slip in segments $H_{n1}^{\min}$ and H_{n2}, the helix angles are equal to (Huang and Vinogradov 1996)

$$\alpha_{n2} = \alpha_{02} + \frac{\sin 2\alpha_0}{2} \frac{P'_2}{K_n} \tag{11}$$

$$\alpha'_{n2} = \alpha'_{02} + \frac{\sin 2\alpha_0}{2} \frac{P'_2}{K_n} \tag{12}$$

In the new slipping segment H_{s2}, the process of a reversed slip will not start until the slip which occurred at the previous stage has been recovered. From the energy conservation principle,

it is equivalent to having double friction forces along the length H_{s2} resisting the new slip. In addition, these forces act in the direction opposite to that at the initial phase. Thus

$$p_{f2}=-2p_f \tag{13}$$

Similarly, when $P'_2>nm_{n2}\cos\alpha_0$, so that micro-slipping occurs along the cable, the friction moments have the following relationship

$$m_{n2}=-2m_n \tag{14}$$

Taking Eq. (14) into account, the helix angle in the new micro-slipping region $H_{n1}^{\min}$ and H_{n2} can be represented, using Eq. (3), as follows

$$\alpha_{m2}=\alpha_{02}+C(P'_2+2nm_n\cos\alpha_0), \tag{15}$$

$$\alpha'_{m2}=\alpha'_{02}+C(P'_2+2nm_n\cos\alpha_0), \tag{16}$$

Furthermore, the helix angle in the new macro-slipping segment can be found to be similar to Eq. (2)

$$\alpha_{s2}=\alpha'_{m2}-\frac{2Dp_f}{\sin\alpha_0}(z-H+H_{n1}^{\min}+H_{n2}),\quad H-H_{n1}^{\min}-H_{n2}\le z\le H \tag{17}$$

Note that the only difference between the unloading and loading phases is in the magnitude and direction of friction forces, as given by Eqs. (13) and (14). Consequently, the relationship between ΔH_{s2} and $\Delta P'_2$, characterising the propagation of the slip during unloading, can be found in a way similar to that in the loading phase. As a result, the length of the reversed slipping segment H_{s2} is found to be directly proportional to the relative load P'_2 in the unloading phase

$$H_{s2}=-\frac{GP'_2}{2p_f} \tag{18}$$

Similar to Eq. (4), the elongation δ'_2, when-$2nm_n\cos\alpha_0\le P'_2\le 0$, is equal to

$$\delta'_2=\frac{4}{\sin 2\alpha_0}\left(\int_0^H \Delta\alpha_{nz}dz+\int_{H_{n1}^{\min}+H_{n2}}^{H}\alpha_{s2}dz\right) \tag{19}$$

which will lead,after substituting Eqs. (9), (11), (14) and (18), to

$$\delta'_2=\frac{2H}{K_n}P'_2-\frac{DG^2}{2\sin^2\alpha_0\cos\alpha_0}\frac{(P'_2)^2}{p_f} \tag{19'}$$

When $P'_2\le$-$2nm_n\cos\alpha_0$, all the non-slipping segments will be in a micro-slipping state, and the elongation is equal to

$$\delta'_2=-\frac{4H}{K_n}nm_n\cos\alpha_0+\frac{4}{\sin 2\alpha_0}\left(\int_0^H \Delta\alpha_{m2}dz+\int_{H_{n2}^{\min}+H_{n2}}^{H}\Delta\alpha_{s2}dz\right) \tag{20}$$

which, after integration, gives,

$$\delta'_2=-\frac{4H}{K_n}nm_n\cos\alpha_0+\frac{4HC}{\sin 2\alpha_0}(P_2+2nm_n\cos\alpha_0)-\frac{DG^2}{2\sin^2\alpha_0\cos\alpha_0}\frac{(P'_2)^2}{p_f} \tag{20'}$$

The actual elongation is equal to the elongation at the beginning of the unloading phase (which is also the elongation at the end of the first loading phase) plus the relative elongation δ'_2, i.e..

$$\delta_2=\delta_1^{\max}+\delta'_2 \tag{21}$$

Since $\delta_1^{\max}$ can be found from Eq. (6) by setting $P_1=P^{max}$ and δ'_2 is given by Eqs. (19) and (20'), the above equation can be expressed as

$$\delta_2=\begin{cases} \dfrac{2H}{K_n}(P_2-P^{\max}+nm_n\cos\alpha_0)+\dfrac{4HC}{\sin 2\alpha_0}(P^{\max}-nm_n\cos\alpha_0)+\dfrac{DG^2}{2\sin^2\alpha_0\cos\alpha_0}\dfrac{[(P^{\max})^2+(2P^{\max}-P_2)P_2]}{p_f} & \text{(I)} \\ -\dfrac{2H}{K_n}nm_n\cos\alpha_0+\dfrac{4Hc}{\sin 2\alpha_0}(P_2+nm_n\cos\alpha_0)+\dfrac{DG^2}{2\sin^2\alpha_0\cos\alpha_0}\dfrac{[(P^{\max})^2+(2P^{\max}-P_2)P_2]}{p_f} & \text{(II)} \end{cases} \tag{22}$$

where formula (I) is applied for $P^{\max}-2nm_n\cos\alpha_0\le P_2\le P^{\max}$ and formula (II) for $0\le P_2\le P^{\max}-2nm_n\cos\alpha_0$. At the end of unloading ($P_2=0$), and the elongation, given by Eq. (22), equals to

$$\delta_2^{\min}=-\frac{2Hnm_n\cos\alpha_0}{K_n}+\frac{4HC}{\sin 2\alpha_0}nm_n\cos\alpha_0+\frac{DG^2}{2\sin^2\alpha_0\cos\alpha_0}\frac{(P^{\max})^2}{p_f}>0 \tag{23}$$

The inequality comes from the observation that the flexibility of the cable with micro-slip ($4HC/\sin^2\alpha_0$) is always larger than that of the cable without any slip ($2H/K_n$). The fact that $\delta_2^{\min}>0$ indicates the existence of a residual elongation at the end of the unloading phase. This is understandable because the interwire resistance force and moment during the unloading becomes twice as large and so a complete recovery of the initially deformed wires cannot be achieved. Note that, during this phase, $d^2\delta_2/dP_2^2<0$, and thus the response curve $\delta_2=\delta_2(P_2)$ is convex (whereas $P_2=P_2(\delta_2)$ is concave).

2.3. Reloading

During the reloading phase the load P_3 increases from 0 to $P^{\max}$. The state at the end of the previous phase, the unloading phase, is taken as the initial state of the cable for the reloading phase.

Fig. 1(d) shows that, at the end of the previous unloading phase, the cable can be characterized by three distinguished segments:

(1) the segment $H_{n1}^{\min}$, in which the helix angle is uniform during the cycle,

(2) the segment $H_{n2}^{\min}$, which experiences macro-slip only once during the first loading phase, and

(3) the segment $H_{s2}^{\max}$, which experiences an alternate macro-slippage. Corresponding initial helix angles in these segments are found, by using Eqs. (15)-(16) and setting $P_2'=-P^{\max}$ and $H_{s2}=H_{s2}^{\max}$, to be

$$\alpha_{03}=\alpha_{02}-C(P^{\max}-2nm_n\cos\alpha_0),\quad 0\le z\le H_{n1}^{\max} \tag{24}$$

$$\alpha'_{03}=\alpha'_{02}-C(P^{\max}-2nm_n\cos\alpha_0),\quad H_{n1}^{\min}\le z\le H-H_{n2}^{\max} \tag{25}$$

$$\alpha''_{03}=\alpha'_{03}-\frac{2Dp_f}{\sin\alpha_0}(z-H+H_{n1}^{\min}+H_{n2}^{\min}),\quad H-H_{n1}^{\min}-H_{n2}^{\min}\le z\le H \tag{26}$$

As expected, when the relative load increases in the reloading phase, a macro-slip, reversed with respect to the previous phase, will start again at the cable ends and then spread to the center. For a symmetrical loading, a new region with a relative slip will not exceed the maximum macro-slipping region of the previous unloading phase, which means that

$$H'_{n3}+H_{s3}=H_{s2}^{\max} \tag{27}$$

Note also that the axial load at the beginning of the reloading phase is equal to zero and thus the relative load at this phase is equal to the absolute value of the load on the cable, namely

$$P_3=P'_3 \tag{28}$$

When the amplitude of P'_3 is so small that there is no slip in segments $H_{n1}^{\max}$, $H_{n2}^{\min}$ and H_{n3}, the helix angles are found, similarly to Eqs. (11)-(12), to be

$$\alpha_{n3}=\alpha_{03}+\frac{\sin2\alpha_0}{2}\frac{P'_3}{K_n} \tag{29}$$

$$\alpha'_{n3}=\alpha'_{03}+\frac{\sin2\alpha_0}{2}\frac{P'_3}{K_n} \tag{30}$$

$$\alpha''_{n3}=\alpha''_{03}+\frac{\sin2\alpha_0}{2}\frac{P'_3}{K_n} \tag{31}$$

These relationships are shown in Fig. 1(d) by the solid lines equally spaced from the dashed lines characterising the initial angles α_{03}, α'_{03} and α''_{03}.

The process of reversed micro- and macro-slip will be similar to that at the unloading phase, so that

$$p_{f3}=2p_f,\qquad m_{n3}=2m_n \tag{32}$$

Note that the difference between the reloading and unloading phases is in the direction of the friction forces and moments (comparing Eq. (32) to Eqs. (13) and (14)). Therefore, the following results can be found by following a similar procedure for the unloading phase:

$$\alpha_{m3}=\alpha_{03}+C(P'_3-2nm_n\cos\alpha_0), \tag{33}$$

$$\alpha'_{m3}=\alpha'_{03}+C(P'_3-2nm_n\cos\alpha_0), \tag{34}$$

$$\alpha''_{m3}=\alpha''_{03}+C(P'_3-2nm_n\cos\alpha_0), \tag{35}$$

$$\alpha_{s3}=\alpha''_{m3}+\frac{2Dp_f}{\sin\alpha_0}(z-H+H_{n1}^{\min}+H_{n2}^{\min}+H_{n3}),\quad H-H_{n1}^{\min}-H_{n2}^{\min}-H_{n3}\le z\le H \tag{36}$$

$$H_{s3}=G_3P'_3,\qquad \text{where } G_3=\frac{G}{2} \tag{37}$$

Similar to Eq. (4), the elongation δ'_3, when $0\le P'_3\le 2nm_n\cos\alpha_0$, is equal to

$$\delta'_3=\frac{4}{\sin 2\alpha_0}\left(\int_0^H \Delta\alpha_{n3}dz+\int_{H-H_{s3}}^H \Delta\alpha_{s3}dz\right) \tag{38}$$

which leads, after substituting Eqs. (34)-(37), to

$$\delta'_2=\frac{2H}{K_n}P'_2-\frac{DG^2}{2\sin^2\alpha_0\cos\alpha_0}\frac{(P'_2)^2}{p_f} \tag{38'}$$

When $2nm_n\cos\alpha_0\le P'_3$, all the non-slipping segments are again in a micro-slipping state, and the elongation becomes

$$\delta'_3=\frac{4H}{K_n}nm_n\cos\alpha_0\frac{4}{\sin 2\alpha_0}\left(\int_0^H \Delta\alpha_{m3}dz+\int_{H-H_{s3}}^H \Delta\alpha_{s3}dz\right) \tag{39}$$

which will lead to

$$\delta'_3=\frac{4H}{K_n}nm_n\cos\alpha_0+\frac{4HC}{\sin 2\alpha_0}(P_3-2nm_n\cos\alpha_0)+\frac{DG^2}{2\sin^2\alpha_0\cos\alpha_0}\frac{(P'_3)^2}{p_f} \tag{39'}$$

The actual elongation is equal to the elongation at the beginning of the reloading phase (which is also the elongation at the end of the unloading phase) plus the relative elongation δ'_3, i.e.,

$$\delta_3=\delta_2^{\min}+\delta'_3 \tag{40}$$

where $\delta_2^{\min}$ is the residual elongation at the end of the unloading phase given by Eq. (23) for $P_2=0$. Thus, using Eqs. (23), (38') and (39'), the actual elongation is found to be

$$\delta_2=\begin{cases}\dfrac{2H}{K_n}(P_3-2nm_n\cos\alpha_0)+\dfrac{4HC}{\sin 2\alpha_0}nm_n\cos\alpha_0+\dfrac{DG^2}{2\sin^2\alpha_0\cos\alpha_0}\dfrac{[(P^{\max})^2+P_3^2]}{p_f} & \text{(I)}\\ \dfrac{2H}{K_n}nm_n\cos\alpha_0+\dfrac{4HC}{\sin 2\alpha_0}(P_3-nm_n\cos\alpha_0)+\dfrac{DG^2}{2\sin^2\alpha_0\cos\alpha_0}\dfrac{[(P^{\max})^2+P_3^2]}{p_f} & \text{(II)}\end{cases} \tag{41}$$

where formula (I) is applied for $P^{\max}-2nm_n\cos\alpha_0\le P_3\le P^{\max}$ and formula (II) for $0\le P_3\le P^{max}-2nm_n\cos\alpha_0$. Note that $d^2\delta_3/dP_3^2>0$, so that the response curve $\delta_3=\delta_3(P_3)$ is concave during the reloading phase (correspondingly, $P_3=P_3(\delta_3)$ is convex).

Obviously, at the end of the reloading phase, where $P_3=P^{max}$, the cable elongation is

$$\delta_3^{\max}=\frac{2H}{K_n}nm_n\cos\alpha_0+\frac{4HC}{\sin 2\alpha_0}(P^{\max}-nm_n\cos\alpha_0)+\frac{DG^2}{\sin^2\alpha_0\cos\alpha_0}\frac{(P^{\max})^2}{p_f} \tag{42}$$

which is the same as that at the end of the first loading phase. Therefore, the load-elongation curve in a cyclic loading will form a hysteretic loop enclosed by the unloading and reloading curves, as shown schematically in Fig. 2. For this reason, in the analysis of cyclic loading the two phases unloading and reloading are of interest, since in an ideal multi-cyclic loading the hysteretic loop will repeat itself.

If only the unloading and reloading phases are important, the residual elongation, shown in Fig. 2, can be excluded from the consideration. It means that Eq. (23) can be subtracted from Eqs. (22) and (41) for unloading and reloading phases. As a result, the load-elongation curves for the cable under cyclic loading will form a closed loop as shown in Fig. 3.

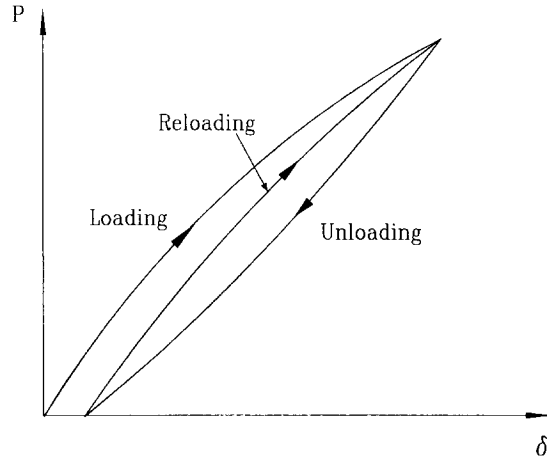

Fig. 2 Scheme of load-elongation relationship during first cycle.

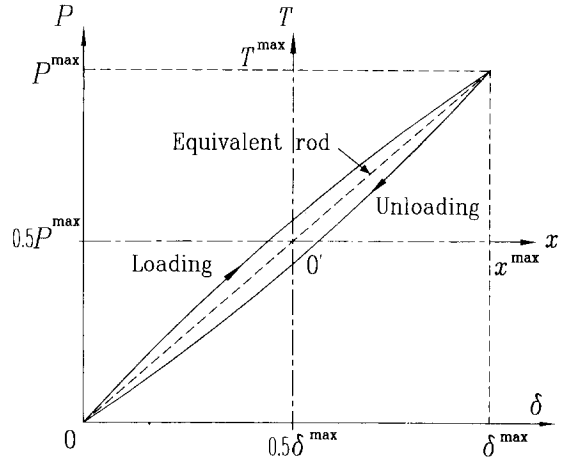

Fig. 3 Hysteretic loop.

2.4. Energy loss per cycle

The energy loss in a half-length of the cable subjected to cyclic loading is defined by

$$W_f = \int P d(\delta_3 - \delta_2) \tag{43}$$

After substitution of expressions for δ_2 from Eq. (22) and δ_3 from Eq. (41), and integration of Eq. (43), the energy loss can be found to be

$$W_f = 8Hnm_n \cos\alpha_0 (P^{max} - 2nm_n \cos\alpha_0)\left[\frac{2C}{\sin 2\alpha_0} - \frac{1}{K_n}\right] + \gamma \frac{(P^{max})^3}{p_f} \tag{44}$$

where

$$\gamma=\frac{2DG^2}{3\sin^2\alpha_0\cos\alpha_0} \tag{45}$$

The constant γ in Eq. (45) depends on structural and material properties of the cable. Eq. (44) indicates a complex energy dissipation model comprising two parts: one is proportional to the axial load and friction moment, and another proportional to the cube of the load amplitude and in inverse proportion to the interwire friction force. The first one is a reflection of friction work, and the second one represents a classical energy dissipation pattern in lap joints (Goodman 1959).

3. Cable as an equivalent rod

As it has been shown above, a model of a cable with finite friction between the wires has nonlinear stiffness characteristics and amplitude-dependent damping properties. In this section a model of a cable as a rod, having material properties such that the properties of a cable and those of the rod are equivalent, is presented. This is done for the simplest situation when a cable in a system serves as a nonlinear spring and dashpot element, so that the inertial properties of the cable can be neglected. An equivalent rod can be found by considering oscillations of a single-degree-of-freedom system, shown in Fig.4. The forced oscillation of this system is governed by the equation of motion

$$m\ddot{x}+T=F\sin\Omega t \tag{46}$$

where F and Ω are the amplitude and frequency of excitation, respectively; x is the elongation of the cable, and T is the force in the cable.

To present the force-displacement relationship in a forced vibration, a symmetric transformation of the force-elongation formulas with $x=\delta-x^{\max}$ and $T=P-T^{\max}$, in which $x^{\max}=\delta^{\max}/2$ and $T^{\max}=P^{\max}/2$ (see Fig. 3), must be done. The maximum elongation in a cyclic process is represented by

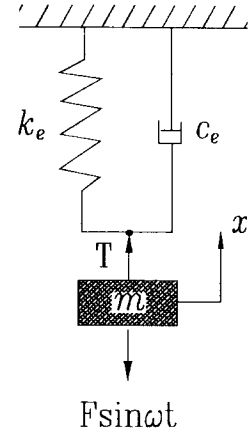

Fig. 4 A spring-dashpot element representing cable in one-degree-of-freedom system.

$$\delta^{\max}=\delta_3^{\max}-\delta_2^{\min} \tag{47}$$

Substitution of Eqs. (23) and (42) into the latter yields the following

$$\delta^{\max}=\frac{4HC}{\sin 2\alpha_0}P^{\max}+4Hnm_n\cos\alpha_0\left(\frac{1}{K_n}-\frac{2C}{\sin 2\alpha_0}\right)+\frac{DG^2}{\sin^2\alpha_0\cos\alpha_0}\frac{(P^{\max})^2}{p_f} \tag{48}$$

The stiffness of the equivalent rod is defined as

$$k_e=\frac{T^{\max}}{x^{\max}}=\frac{P^{\max}}{\delta^{\max}} \tag{49}$$

According to Eq. (48), the latter can be represented by

$$k_e=\frac{1}{\frac{4HC}{\sin 2\alpha_0}+\frac{4Hnm_n\cos\alpha_0}{P^{\max}}\left(\frac{1}{K_n}-\frac{2C}{\sin 2\alpha_0}\right)+\frac{DG^2}{\sin^2\alpha_0\cos\alpha_0}\frac{P^{\max}}{p_f}} \tag{50}$$

Since the friction moment m_n at the contact patches is small, the corresponding term in the denominator in Eq. (50) can be neglected in most engineering applications. With this approximation, the equivalent stiffness becomes

$$k_e\approx\frac{1}{\frac{4HC}{\sin 2\alpha_0}+\frac{DG^2}{\sin^2\alpha_0\cos\alpha_0}\frac{P^{\max}}{p_f}} \tag{51}$$

which is a nonlinear function of the amplitude of the cyclic load.

The damping coefficient in the equivalent rod can be found by equating the energy dissipation per cycle in the ideal system to the actual one. That is

$$W_f=c_e\pi\Omega(x^{\max})^2 \tag{52}$$

Representing $x^{\max}$ by $P^{\max}/2k_e$ and using the result of Eq. (50), the equivalent damping coefficient is found to be

$$c_e=\frac{4k_e^2}{\pi\Omega}\left[\frac{8Hnm_n\cos\alpha_0}{P^{\max}}\left(1-\frac{2nm_n\cos\alpha_0}{P^{\max}}\right)\left(\frac{2C}{\sin 2\alpha_0}-\frac{1}{K_n}\right)+\gamma\frac{P^{\max}}{P_f}\right] \tag{53}$$

Again, neglecting the small term with $(nm_n\cos\alpha_0/P^{\max})^2$, Eq. (53) can be approximated by

$$c_e\approx\frac{4k_e^2}{\pi\Omega}\left[\frac{8Hnm_n\cos\alpha_0}{P^{\max}}\left(\frac{2C}{\sin 2\alpha_0}-\frac{1}{K_n}\right)+\gamma\frac{P^{\max}}{P_f}\right] \tag{54}$$

As it is seen, both k_e and c_e are nonlinear functions of the amplitude of cyclic loading. These function are shown qualitatively in Figs. 5 and 6.

4. Examples

In this section some numerical examples are given to demonstrate the theory and present some results. The structural data for a single layered cable given by Utting and Jones (1987)

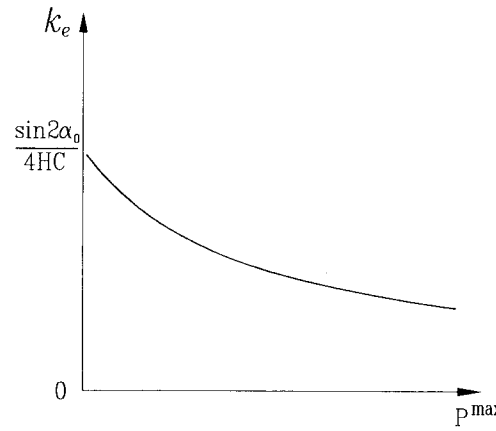

Fig. 5 Equivalent stiffness *vs* amplitude of oscillation relationship.

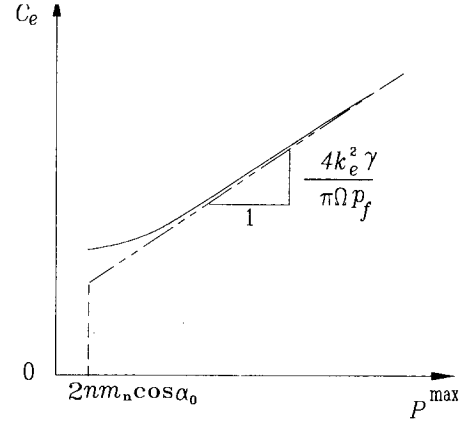

Fig. 6 Equivalent damping *vs* amplitude of oscillation relationship.

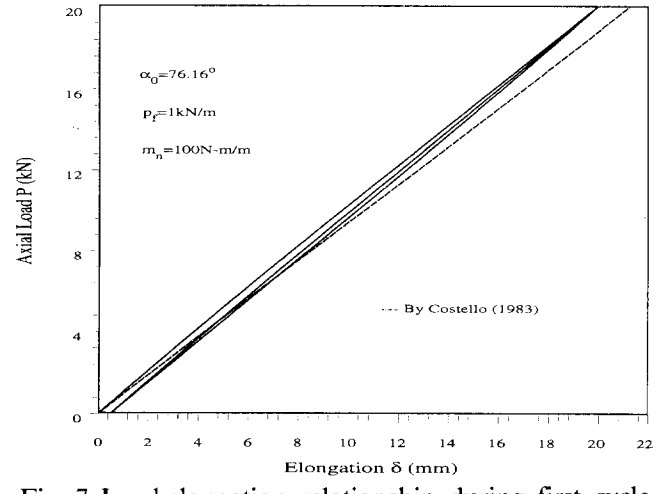

Fig. 7 Load-elongation relationship during first cycle.

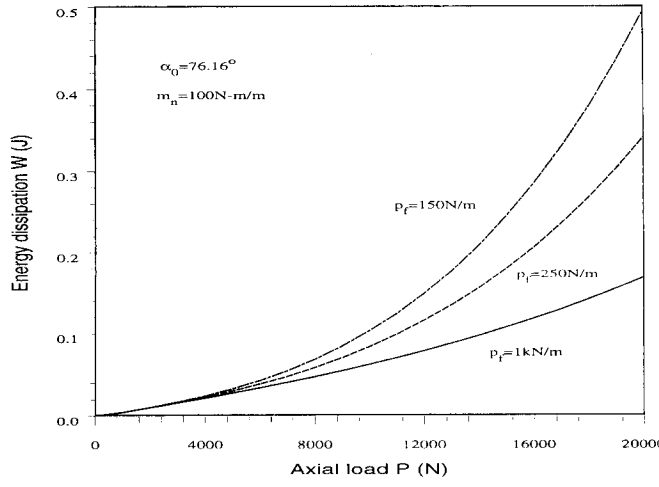

Fig. 8 Energy dissipation per cycle-the influence of friction forces.

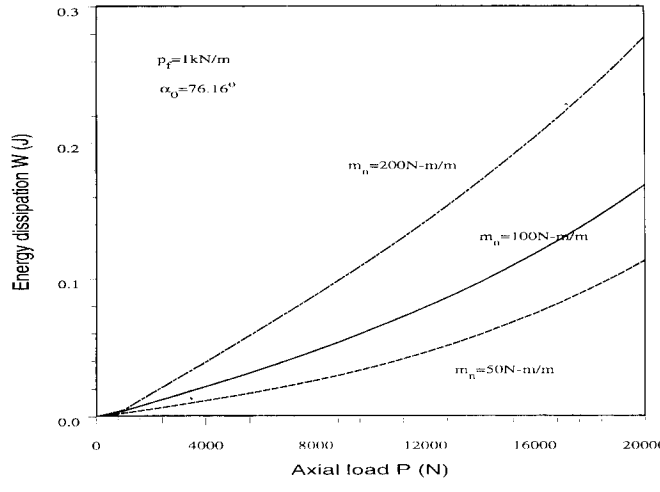

Fig. 9 Energy dissipation per cycle-the influence of friction moment.

are used, specifically, $n=6$, $R_c=1.97$ mm, $R=1.865$ mm, $\alpha_0=76.16°$, $H=0.75$ m, $E=E_c=197.9$ GPa, $\nu=\nu_c=0.3$, and the interwire distributed friction force and moment are assumed to be constant and respectively equal to 1 kN/m and 100N-m/m, except when indicated otherwise.

The elongation of the cable during a cycle of loading is shown in Fig. 7, where one can see a closed loop formed by the unloading and reloading curves. The enclosed area indicates, therefore, the energy losses during the cycle. The broken line is shown for the case of the friction-free cable (Costello's model). Note that due to the interwire slip the cable's elongation is not equal to zero at the end of the unloading phase.

Eq. (44) indicates that the energy dissipation per cycle which is caused by two sources, micro-slip and macro-slip, has, correspondingly, two components, one, proportional to the first power

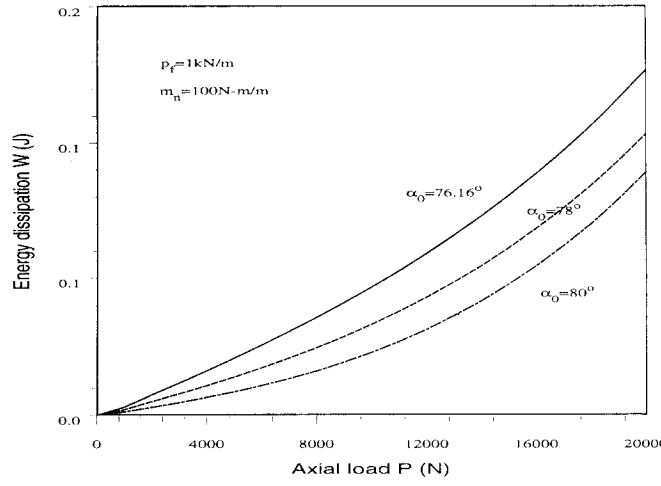

Fig. 10 Energy dissipation per cycle-the influence of helix angle.

of the force amplitude, and the other, to the third power. The latter component is analogous to the type of relationship characterising energy dissipation in the lap joints (Goodman 1959). In Fig. 8 and 9 the influence of friction forces and moments, and in Fig.10 the effect of the helix angle on energy losses are shown. Note, that smaller helix angles lead to larger energy losses.

5. Conclusion

For a model of a cable comprising a core and wound around it wires, a theory of cyclic axial deformations in the presence of dry friction is developed. Explicit load-elongation relationships are obtained for the loading, unloading and reloading phases of the cycle. It is shown that these relationship are weakly nonlinear. It is also shown that the unloading and reloading phases of a symmetric cycle form a closed loop characterising the structural losses in a cable. Explicit expression for these losses is derived, which comprises two components: one due to the micro-slippage at the contact patches, and another due to the propagation of the macro-slippage along the cable.

It is suggested that in applications where inertial properties of the cable can be neglected a model of it as a solid rod with amplitude-dependent damping properties can be used. Using the equivalent linearization technique, explicit expression for the equivalent coefficient of damping is derived. The numerical examples show the presence of residual strains in a cyclically loaded cable, and also the effect of friction forces and moments and the helix angles on structural losses.

Acknowledgements

The financial support provided by the Natural Sciences and Engineering Research Council

of Canada in the form of an operating grant is gratefully acknowledged.

References

Costello, G. A. (1983), "Stresses in multilayered cables", *Proc. 2nd Int. Offshore Mech. and Arctic. Engrg.*, New York, 355-359.

Huang, X. and Vinogradov, O. G. (1992), "Interwire slip and its influence on the dynamic properties of tension cables", *2nd International Offshore and Polar Engineering Conference*, Paper No. ISOPE-92-T5-01, San Francisco, USA, June 14-19.

Huang, X. and Vinogradov, O.G. (1994), "Analysis of dry friction hysteresis in a cable under uniform bending", *Structural Engineering and Mechanics*, **2**(1), 63-80.

Huang, X. and Vinogradov, O.G. (1996), "Extension of a cable in presence of dry friction", *Structural Engineering and Mechanics* **4**(3), 313-329.

Goodman, L. E. (1959), "A review ot progress in analysis of internal slip damping", *Structural Damping*, Ruzicka, J.E. ed., *ASME*, New York, 35-48.

Utting, W. S., and Jones, N. (1987), "The response of wire rope strands to axial tensile loads part I: Experimental results and theoretical predictions", *Int. J. Mech. Sci.*, **29**(9), 605-619.

Vinogradov, O. G., and Atatekin, I. S. (1986), "Internal friction due to twist in bent cable", *J. of Eng. Mech., ASCE*, **112**(9), 859-873.